In vitro investigation of the suitability of restorative and implant materials for the prevention of dental implant associated infections

Doctoral Thesis

Ágnes Györgyey

Semmelweis University

PhD School of Basic and Translational Medicine

Consultant: Zsombor Lacza, MD, DSc

Official Reviewers:	Rita Kiss, DSc Árpád Joób-Fancsaly. DMD, PhD
Head of the Complex Examination Committee:	Barna Vásárhelyi, MD, DSc
Members of the Complex Examination Committee:	Péter Andréka, MD, PhD Ákos Zsembery, MD, PhD

Budapest

2020

1 INTRODUCTION

One of the leading causes of the failure of titanium dental implants is related to implant-associated bacterial infections (peri-implantitis). Since the current medical technologies are not efficient in the curative treatment of peri-implantitis the prevention of the infections provides a plausible alternative strategy. One strategic approach has been the improvement of the biocompatibility of dental implants ensuring complete biological sealing around the implant in order to exclude pathogenic bacteria from the implant site. A more recent approach is the enhancement of the antibacterial feature of the surface of dental implants with the view to create an 'active' line of defence against bacterial infections. In my doctoral work I investigated the practical aspects of these two strategic approaches in *in vitro* experiments.

2 OBJECTIVES

2.1 Investigation of the *in vitro* biocompatibility of prosthetic materials with human epithelial cells

2.2 Investigation of the *in vitro* biocompatibility of laser ablated TiO_2 surfaces

2.3 Investigation of the *in vitro* antibacterial property of nanocomposite polymers

3 MATERIALS AND METHODS

3.1 *In vitro* biocompatibility of prosthetic materials with human epithelial cells

3.1.1 Preparation of samples of prosthetic materials

Cylindrical samples of 1.5 mm height and 9 mm diameter were prepared from lithium-disilicate, yttrium modified zirconium dioxide and CoCr alloy. The experiments with human epithelial cells were carried out on 5 samples per type at a time and experiments were repeated 4 times (Table 1).

Table 1. Clinical relevance of the selected test materials.

Material	Clinical role
CoCr alloy	Base material of porcelain fused metal crowns which is the most often used material for fixed (crown and bridge) restorations
Lithium-disilicate	Most frequently used metal-free aesthetic material for crown and short bridge restorations
Yttrium modified zirconium dioxide	It is used as restorative and implant material, as well. It is a metal free solution for crowns and even full arch bridges.

3.1.2 Investigation of the proliferation of epithelial cells on prosthetic materials

Adult epidermal epithelial cells were isolated and cultured from inflammation-free oral mucosa of a healthy donor (age 18–46) undergoing dento-alveolar surgery. Cells were cultured on the samples of prosthetic materials in 48-well plates at a density of 10^4 cells/well. AlamarBlue assay

was used to follow-up the quantity of living cells. As positive control, the proliferation of cells was measured in culture plates (data not shown).

3.1.3 Statistical analysis

The proliferation of adhered cells was expressed as the percentage change in the reduction of AB, which was calculated from the OD_{570} and OD_{600} values for each well. After normality testing the data were compared via one-way analysis of variance (ANOVA), followed by the LSD, Sidak and Dunnett post hoc tests. Comparison of the 24h (attachment) and 72 h (proliferation) observations was carried out with Student's t-test for paired samples. A probability value of $p < 0.05$ was considered as statistically significant.

3.2 *In vitro* biocompatibility of laser ablated TiO_2 surfaces

3.2.1 Preparation of samples

For the experiments 1.5 mm thick, 9 mm in diameter discs were cut from commercially pure (CP4) titanium rods. After degreasing the discs were subjected to sandblasting with aluminium oxide of 150 μm grain size and then to acid etching with nitric acid. A frequency-doubled Q-switched Nd:YAG laser (λ = 532 nm, FWHM = 10 ns) was used for the ablation of titanium discs (n = 80). The applied fluence was 1.3 J/cm^2. A 3.6 mm^2 area on the sample surface was illuminated by a series of 200 laser pulses under atmospheric conditions. Further experiments were performed with a ns KrF excimer laser beam (λ = 248 nm, FWHM = 18 ns). The applied fluence on the titanium

surface was 0.4 J/cm^2, the illuminated area was 10.5 mm^2 and the number of pulses was 2000 under atmospheric conditions. In total, 80 discs were treated.

3.2.2 Cell culture experiments on laser ablated TiO_2 surfaces

Osteoblast-like MG-63 cells were seeded in 48-well cell culture plates onto each disc at a density of 10^4. The cell adhesion was measured at 24h and the cell proliferation at 72h. MTT and Alamar Blue (AB) assays were used to determine the quantity of living cells. The optical density of the reduced MTT solution at 540 nm (OD_{540}) was determined. OD_{570} and OD_{600} were measured to determine the reduction of AB. Four parallel experiments were performed, and 5 samples were used for each treatment and for each assay. Osteogenic differentiation was also investigated on laser ablated surfaces. Alkaline phosphates (ALP) activity was determined by the hydrolysis of p-nitrophenyl phosphate in 2-amino-2-methyl-1-propanol buffer. Absorbance was measured at 504 nm wavelength with spectrophotometry.

3.2.3 Statistical analysis

For the MTT method, the mean $OD_{540} \pm \sigma_{\bar{x}}$ is given. In the AB method, the percentage reduction of AB was calculated from the OD_{570} and OD_{600} data by the given protocol. After normality testing the data were compared via one-way analysis of variance (ANOVA), followed by the LSD, Sidak and Dunnett post hoc tests. A probability value of $p < 0.05$ was considered to be statistically significant.

3.3 *In vitro* antibacterial property of nanocomposite polymers

3.3.1 Experimental groups

Six experimental groups were created as follows (Table 2): in group A, acid-etched and sand-blasted titanium discs were used as control. In group B, the acid-etched and sand-blasted discs were coated with poly(ethyl acrylate-co-methyl methacrylate (p(EA-co-MMA)) polymer. In group C, the discs were covered with p(EA-co-MMA polymer containing TiO_2 photocatalyst. In group D, the TiO_2-polymer composite was supplemented with dodecyl-sulphate (DS). In group E, nanoAg-TiO_2 photocatalyst was dispersed in the coating polymer. The mixture contained 0.5 wt% surface silver nanoparticles. In group F, the nanoAg-TiO_2 polymer composite was supplemented with DS (Figure 1).

In order to investigate the photocatalysis mediated antibacterial property of the polymer nanohybrid coatings, the experimental groups were further divided into 'light' and 'dark' sets. In the 'light' set the discs were irradiated for 10 minutes at 37°C with UV-VIS light source using a 15W low-pressure mercury lamp with an intensity of 1.26×10^{-6} einstein/s in the VIS range with characteristic emission wavelengths mostly above 435 nm. However, it also had emission lines at 254, 353 and 393 nm, but the intensity of these lines is significantly lower compared to that of visible range wavelengths (data not shown). In the 'dark' or 'control' set the discs were kept in the dark at 37°C. Before irradiation the supernatant was removed from the wells and replaced with 0.2 ml phosphate buffer saline medium. After irradiation 10% 1 mg/ml MTT solution was added to the PBS solution. Following 4h incubation under standard conditions at 37°C the medium was

gently removed from each well and the crystallized formazan dye was solubilized in absolute isopropanol supplemented with 0.04M HCl and 10% sodium dodecylsulfate. The optical density of the solution was determined at 540 nm. Four (4) parallel experiments were performed including 4 samples per each experimental group as it is shown in Table 2.

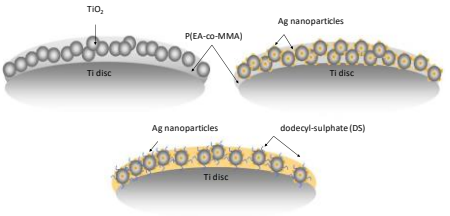

Figure 1 shows the schematic drawings of the NP containing surfaces.

Table 2. Experimental groups. Dark set comprises the number of samples that were kept in dark, while light set comprises the number of samples that were subjected to UV-VIS irradiation in each experimental group.

Surface types	Group	Dark set	Light set
Sandblasted and acid-etched surface	(A)	n=16	n=16
p(EA-co-MMA) copolymer	(B)	n=16	n=16
60wt% TiO_2 : 40wt% copolymer	(C)	n=16	n=16
60wt% DS-TiO_2 : 40wt% copolymer	(D)	n=16	n=16
60wt% Ag-TiO_2 : 40wt% copolymer	(E)	n=16	n=16
60wt% Ag-DS/TiO_2 : 40wt% copolymer	(F)	n=16	n=16

3.3.2 Isolation and characterization of *S. salivarius*

S. salivarius was chosen as a model bacterium for the experiments because of its significant role as a primary colonizer in peri-implantitis. The characterization of the strain was performed with Microflex LT MALDI-TOF mass spectrometer.

3.3.3 Antibacterial activity of Ag/TiO_2/polymer nanohybrid coatings

S. salivarius was introduced into 0.5 ml reduced BHI broth in a density adjusted to McFarland standard 0.5. The bacteria were cultured with the coated and the control discs in 48 well plates for 4 hours under standard conditions at 37°C. The growth of *S. salivarius* on the surface of the discs was measured by MTT assay.

3.3.4 Statistical analyses

Data was grouped according to the applied surface treatment and whether the surface was irradiated or not. For data exploration, group means and their 95% confidence intervals were calculated using appropriate t-distributions centered at the sample mean of a given measurement group, with standard deviation equal to the standard error of the measurement within the group and degrees of freedom equal to the sample size in the group less one. Absorbance values were further analysed to isolate the effects of the different surface treatments and the effect of irradiation on absorbance levels.

Comparisons were made within treatment groups between irradiated and dark samples as well as across treatment groups. Due to the large number of comparisons and the highly different variances across groups a Bayesian multilevel linear model was used for the analysis.

4 RESULTS

4.1 *In vitro* biocompatibility of prosthetic materials with human epithelial cells

4.1.1 Cell attachment and proliferation on prosthetic materials

At 24-h, significant difference was found between the attachment on zirconium-dioxide and Li-disilicate samples ($p < 0.045$ according to all post hoc tests), and Li-disilicate showed the highest attachment among the restorative materials (Figure 2). There was a significant increase in every group comparing the 24-h and the 72-h results.

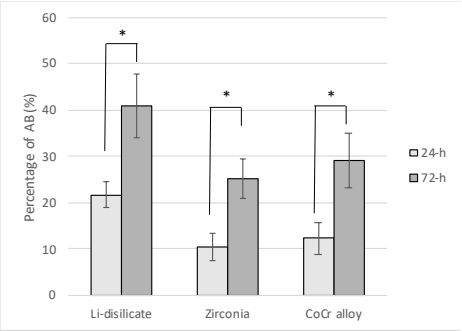

Figure 2 shows the 24-h and the 72-h percentage reduction of AB on the Li-disilicate, zirconia and CoCr alloy samples. After 24 hours, the mean percentage reduction of AB was 21.7 ± 2.8% for the Li-disilicate sample, 10.5 ± 3.0% for the zirconia samples and 12.3 ± 3.4% for the CoCr alloy sample. After 72h the reduction was 40.9 ± 7.0% for the Li-disilicate sample, 25.2 ± 4.3% for the zirconia sample, and 29.1 ± 5.9% for the CoCr alloy sample. The comparison of the 24-h (attachment) and 72-h (proliferation) resulted in the following values: Li-disilicate: ($p = 0.011$), zirconia: ($p = 0.032$), CoCr: ($p = 0.015$).

4.2 *In vitro* biocompatibility of laser ablated TiO_2 surfaces

4.2.1 Cell attachment investigated by SEM

Figure 3A-C shows the SEM images of the attached MG-63 osteoblast-like cells on different titanium surfaces after 24-h culturing. SEM did not reveal any morphological differences on cells either on control or treated titanium surfaces.

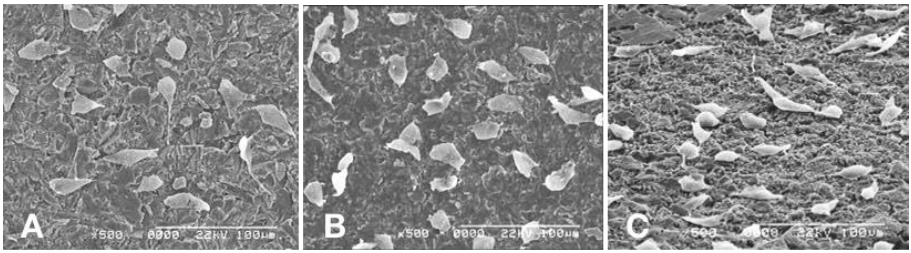

Figure 3 shows representative SEM images of MG-63 osteoblast-like cells (24-h observation) on (A) an acid-etched and sand-blasted Ti surface (control), (B) a Nd:YAG laser-ablated Ti surface and (C) a KrF excimer laser-ablated Ti surface. Magnifications: 500x. Image (B) shows unpublished data.

4.2.2 Cell attachment and proliferation on laser ablated TiO_2 surfaces

4.2.2.1 MTT assay

The results of MTT measurements relating to cell attachment (24-h observation) and cell proliferation (72-h observation) are illustrated in the bar graphs of Figure 4. No statistical differences were observed between the groups after the 24-h observation. The MTT data indicated that the MG-63 osteoblast-like cell proliferation on all the Ti surfaces was statistically significantly enhanced at 72-h relative to the cell attachment at 24-h ($p < 0.05$). No significant differences were observed between the groups after the 72-h proliferation.

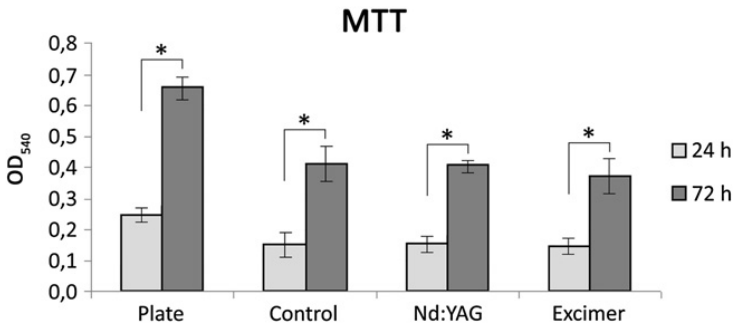

Figure 4 shows of MTT after 24-h and 72-h on the plate, on the control samples, on the Nd:YAG laser-irradiated samples and on the excimer laser-treated samples. The mean ± $\sigma_{\bar{x}}$ of the OD_{540} values observed after 24-h observation were 0.246 ± 0.024 for the cells seeded on the plate itself, 0.150 ± 0.040 for the control sample, 0.153 ± 0.026 for the Nd:YAG laser-treated samples, and 0.146 ± 0.024 for the excimer laser-treated sample. The mean ± $\sigma_{\bar{x}}$ of the OD_{540} values observed after 72 h were 0.656 ± 0.037 on the plate, 0.410 ± 0.056 for the control sample, 0.403 ± 0.020 for the Nd:YAG laser-treated sample, and 0.372 ± 0.059 for the excimer laser-treated sample.

4.2.2.2 AlamarBlue assay

The percentage reduction was calculated from the OD_{570} and OD_{600} values for each well, as recommended in the protocol provided by the manufacturer. No statistical differences were observed between the groups after the 24-h observations. The 72-h observations revealed statistically significantly enhanced cell proliferation on all the surfaces relative to the cell attachment ($p < 0.05$). No significant differences were observed between the groups after the 72-h proliferation (Figure 5).

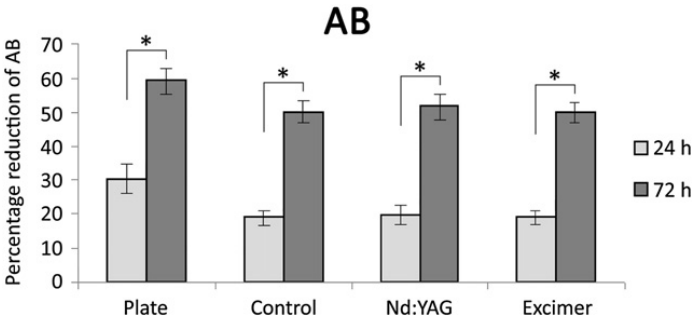

Figure 5 shows percentage reduction of AB after 24-h and 72-h on the plate, on the control samples, on the Nd:YAG laser-irradiated samples and on the excimer laser-treated samples. After 24 h, the mean percentage reduction of AB was 30.36% ± 4.15% on the plate, 18.95% ± 2.21% for the control sample, 19.80% ± 2.64% for the Nd:YAG laser-treated samples and 19.09% ± 2.06% for the excimer laser-treated sample. After 72 h the reduction was 59.20% ± 3.56% on the plate, 49.91% ± 3.29% for the control sample, 51.69% ± 3.83% for the Nd:YAG laser-treated sample, and 49.87% ± 3.22% for the excimer laser treated sample.

4.2.3 Cell differentiation on laser ablated TiO_2 surfaces

The results of the differentiation tests are represented in Figure 6. Statistically ($p < 0.05$) a decreased secretion of ALP was observed on the Nd:YAG surface treated samples compared to the control ones. These data indicated that after 7 days of incubation, no statistical differences in the secretion of ALP were seen between the control and the laser-treated groups.

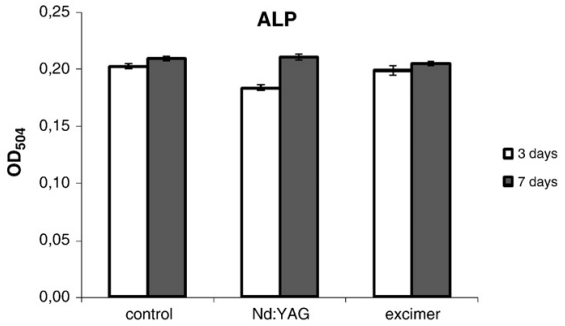

Figure 6 shows ALP activity (OD_{504}) after 3-days and 7 days observation on the control samples, the Nd:YAG laser-irradiated samples and the excimer laser-treated samples. The mean ± $\sigma\bar{x}$ of the OD_{504} values of the 3-day observation was 0.203 ± 0.002 for the control sample, 0.184 ± 0.003 for the Nd:YAG laser-treated samples, and 0.199 ± 0.004 for the excimer laser-treated sample. The mean ± $\sigma\bar{x}$ of the OD_{504} values of the 7 day observations was 0.210 ± 0.002 for the control sample, 0.211 ± 0.003 for the Nd:YAG laser-treated sample, and 0.205 ± 0.002 for the excimer laser-treated sample.

4.3 *In vitro* antibacterial property of nanocomposite polymers

The characterization of the clinical isolate of bacterium strain, the MALDI-TOF MS gave a species level identification with log(score)=2.184 for *S. salivarius* strain.

Absorbance levels (MTT) had distinct group means across most treatment and irradiation conditions as suggested by the minimal overlap in the confidence intervals (Figure 7). The linear decomposition of the absorbance levels into surface effects, surface-based irradiation effects and noise yielded comparative results. Under dark conditions, the group means of absorbance in the TiO_2 photocatalyst containing (C) and (D) experimental groups was higher than those of the Ag/TiO_2/polymer nanohybrid films in the

(E) and (F) groups. This suggests that more *S. salivarius* attached to the surface of TiO_2 containing polymer films than to Ag/TiO_2/polymer nanohybrid films. The mean absorbance in the (E) and (F) groups was credibly lower than in any of the other groups. The control (A) group had the highest mean absorbance of all groups, being credibly higher than (B) and (D) but compared to group (C) a zero difference still falls in the 95% credible interval.

The net effect of UV-VIS irradiation on absorbance values was negative in each group (95% CI excluded zero), indicating that the viability of bacteria was reduced on the irradiated surfaces. The same tendency was observed on the control surface (A) after irradiation than in C, D and E, F experimental groups. However, this reduction was the lowest in the (B) experimental group where the control surface was coated with p(EA-co-MMA) polymer without any photocatalyst content. In absolute magnitude the highest irradiation effect of -0.15 $CI_{95\%}$(0.09, 0.21) was observed in the (C) group, while relative to the dark levels the (E) group showed the largest percentage change of 60% $CI_{95\%}$(50%, 67%), followed by group (C) 33% $CI_{95\%}$(23%, 42%). The credible differences are presented on Figure 8.

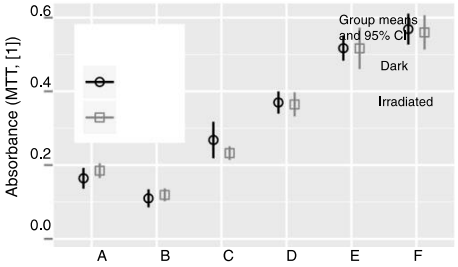

Figure 7 shows the mean MTT absorbance values before and after UV-Vis irradiation. The lack of overlap suggests significant differences between certain groups; however, due to the apparent differences in variances, a Bayesian analysis was used to confirm this.

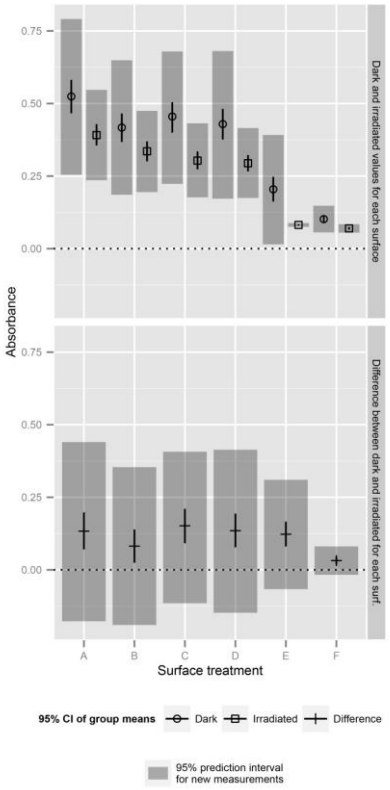

Figure 8 shows the credible intervals of absorbance across surface types and irradiation conditions and credible differences between irradiated and dark samples within the same surface types. 95% CIs of group means and individual measurements are displayed.

In brief, our results showed that restorative materials had good *in vitro* biocompatibility with oral mucosa derived epithelial cells. Laser ablation did not improve the biocompatibility of TiO_2 surfaces with MG-63 cells compared to the control sandblasted/acid-etched surfaces. TiO_2 and silver coupled TiO_2 containing nanocomposite polymers showed significant photocatalytic antibacterial property after UV-VIS irradiation. Silver coupled TiO_2 nanocomposite polymer showed contact *in vitro* antibacterial property without irradiation. Surprisingly, the control sandblasted/acid-etched TiO_2 surfaces showed some UV-VIS irradiation induced antibacterial property, too.

5 CONCLUSIONS

5.1 Prosthetic materials show good *in vitro* biocompatibility with human mucosa derived epithelial cells; they might be suitable to support the prevention of primary peri-implantitis.

5.2 Laser ablated TiO_2 surfaces do not show superior *in vitro* biocompatibility compared to the conventional SLA surfaces; they might not be suitable to support the prevention of secondary peri-implantitis by the enhancement of the secondary implant stability.

5.3 Silver and TiO_2 embedded nanocomposite polymers show good photo-induced *in vitro* antibacterial property on the surface of titanium samples; they might become promising candidates to support the prevention of the development of secondary peri-implantitis.

6 PUBLICATION LIST

Publications related to the present thesis

1. **Györgyey Á**, Janovák L, Ádám A, Kopniczky J, Tóth KL, Deák Á, Panayotov I, Nagy K, Cuisinier F, Dékány I, Turzó K. (2016) Investigation of the *in vitro* photocatalytic antibacterial activity of nano-crystalline TiO_2 and coupled TiO_2/Ag containing copolymer on the surface of medical grade titanium.
   J Biomater Appl, 31(1): 55-67.

   IF: 2,31

2. Forster A, Ungvári K, **Györgyey Á**, Kukovecz Á, Turzó K, Nagy K. (2014) Human epithelial tissue culture study on restorative materials.
   J Dent, 42(1): 7-14.

   IF: 2,749

3. **Györgyey Á**, Ungvári K, Kecskeméti G, Kopniczky J, Hopp B, Oszkó A, Pelsőczi I, Rakonczay Z, Nagy K, Turzó K. (2013) Attachment and proliferation of human osteoblast-like cells (MG-63) on laser-ablated titanium implant material.
   J Mat Sci Eng C, 33(7): 4251-4259.

   IF: 2,736